Jarrah Ali Al-Tubaikh

Internal Medicine

An Illustrated Radiological Guide

Second Edition

Springer

Internal Medicine

Jarrah Ali Al-Tubaikh

Internal Medicine

An Illustrated Radiological Guide

Second Edition

Springer

Jarrah Ali Al-Tubaikh
Department of Clinical Radiology
Amiri Hospital – Kuwait City
Kuwait City, Kuwait

All illustrations marked with ❦ were drawn by the author.

ISBN 978-3-319-39746-7 ISBN 978-3-319-39747-4 (eBook)
DOI 10.1007/978-3-319-39747-4

Library of Congress Control Number: 2016954639

Printed on acid-free paper

This Springer imprint is published by Springer Nature
The registered company is Springer International Publishing AG Switzerland

Preface

It is a privilege to write another introduction to this book. When I wrote this book in Munich in 2010, I knew I was writing a book with an uncommon combination, linking internal medicine to radiology. I can still remember the comment of my mentor Prof. Maximillian Reiser after he saw the manuscript's content. He told me: "Why did you choose this layout and these disorders in particular?" I replied: "They are the most commonly encountered diseases daily in any busy medical department."

Over the years, I have noticed how the chapter's download numbers are increasing in Springer's official website. This reflects, to me at least, the continuous demand for such topics worldwide, especially among newly coming radiologists. They are the ones facing the fire daily in duties and emergency calls from physicians and surgeons around the clock. Moreover, radiology board teachings concentrate more and more over emergency cases, trauma cases, postoperative complications, and cancer screening and monitoring. I can assure you that almost 90 % of any radiologist's daily routine lies within one or more of the past four areas in radiology. Internal medicine disorders and complications are considered extracurriculum, and maybe special interest radiology.

Within the past 5 years since the publication of this book, I have noticed a skyrocketing increase in the radiological referrals through my work in two different hospitals. Sometimes, we get radiological referral for simple disorders that do not need radiological investigation, for example, more and more demands for ultrasound to exclude inguinal hernias, ultrasound for lipoma, CT for acute appendicitis suspicion, polytrauma PAN-CT, etc. As a radiologist, it is always nice to be needed; however, technology can be a double-edged sword, reducing the clinical experience of both the referring clinician and the radiologist. Many physicians, unfortunately, started to use radiology as a substitute for clinical examination and judgment. Although such a phenomenon is not necessarily widely found, it is there, no doubt about it.

I am pleased that the first edition of my book has helped many physicians I know to change their perspective toward radiological investigations. I have been contacted by many physicians here in Kuwait and outside of Kuwait who thank me for detailing what they should order and how to investigate certain diseases. In the same fashion, many radiologists are pleased with the variety of images that detail the medical disorders and facilitate their detection.

Based on the past positive feedbacks, I aimed to expand the range of the book by including three more medical fields, which are not directly linked to internal medicine but however are important to know. The second edition of this book exposes the reader to occupational medicine and toxicology, which are uncommonly seen as cases of attempting suicide and accidental intoxications. The radiological literature is filled with different radiological signs reported by many researches detailing intoxications, which have become of great interest since the data are accumulating over the years.

Chiropractic and osteopathic medicine are two important fields that emerged more than a hundred years ago, and they are rarely, if ever, mentioned or taught in medical schools or board-certification programs, especially in specialties related to the orthopedics or the spine. Although they are not considered part of conventional medicine, both specialties have very solid neuroanatomical and neuropathophysiological basis. Chiropractic medicine in particular, founded by D. D. Palmar and perfected by B. J. Palmar, uses radiology as an essential part of its diagnostic techniques. Their radiographic imaging techniques are known as "spinography." Personally, I have been using their radiographic techniques in an extensive fashion to diagnose lower back pain and kinesiological disorders. Their radiological imaging techniques proved to be very valid and very accurate in diagnosing lower back pain, especially lumbar spine MRI with almost normal findings. Unfortunately, such radiological knowledge is very rarely encountered in commonly known radiological journals. I sincerely hope that the reader will find the chapter of chiropractic medicine imaging interesting and informative.

Lastly, a very new medical specialty is arising within the past 5 years: energy and quantum medicine. Although it started with the book *What Is Life?* (1944) by the Nobel Prize winner Austrian physicist Erwin Schrödinger, many new medical and biological researchers are now using quantum physics to define life, including Robert O. Becker, Jerry Tennant, Hans-Peter Dürr, Fritz-Albert Popp, Mae-Wan Ho, and so many others. Their

works have now evolved to so many applications, emerging as unconventional therapies that use waves and frequencies to heal, such as pulsed electromagnetic field (PEMF) therapy, microcurrent therapy, phototherapy, and ultrasonic therapy. I have been personally using these devices for myself and my relatives and for special cases in the hospital, with a high success rate of controlling diseases and complications. I documented my findings on radiological images, imaging patients before and after such unconventional, energetic therapy to find out what has been changed in the disease status radiographically. I took the opportunity of publishing the second edition of this book to introduce the reader to a whole new world that uses therapies based on biophysics rather than biochemistry for conventional, pharmacological medicine uses.

In conclusion, I hope for the reader an interesting journey through the book, and I hope that this book can help someone somewhere in the world save a life.

Jarrah Ali Al-Tubaikh, MD
Kuwait City, Kuwait

Contents

Gastroenterology

J.A. Al-Tubaikh, *Internal Medicine*, DOI 10.1007/978-3-319-39747-4_1

1.1 Liver Cirrhosis

Liver cirrhosis is a term used to describe the histological development of regenerative hepatic nodules surrounded by fibrous bands in response to chronic liver injury.

Cirrhosis is an advanced, diffuse stage of liver injury, which is characterized by replacement of the normal liver parenchyma by collagenous scar (fibrosis). Cirrhosis is accompanied by diffuse distortion of the hepatic vasculature and architecture, resulting in vascular disturbance between the portal veins and the hepatic veins, plus porta hepatic fibrosis. The major cirrhosis consequences are hepatic function impairment, increased intrahepatic resistance (portal hypertension), and the development of hepatocellular carcinoma (HCC).

Types of Liver Cirrhosis

- *Laennec's cirrhosis* is a type of micronodular liver cirrhosis that is seen in patients with malnutrition, alcoholism, or chronic liver steatosis.
- *Posthepatitic cirrhosis* is a micro- and/or macronodular liver cirrhosis commonly seen in patients with hepatitis C virus or uncommonly B virus.
- *Postnecrotic cirrhosis* is macronodular liver cirrhosis that can arise due to fulminating hepatitis infection or due to toxic liver injury.
- *Primary biliary cirrhosis* (*PBC*) (*vanishing bile duct syndrome*) is an autoimmune disease of unknown origin characterized by progressive intrahepatic bile duct, nonsuppurative inflammation, and destruction by T-cell lymphocytes, which leads later on to micronodular liver cirrhosis, hepatomegaly, with greenish-stain liver on gross examination due to bile retention. PBC occurs in middle-aged women in up to 90 % of cases. In symptomatic PBC, patients may complain of jaundice in the first 2–3 years, which develops later into portal hypertension and hepatosplenomegaly. In the asymptomatic PBC, the only symptom is abnormal serum hepatobiliary enzyme levels. PBC is classified pathologically into four main stages. *Florid duct stage* (*stage I PBC*) is characterized by vanishing intrahepatic duct and ductopenia due to destruction of the intrahepatic bile duct basement membrane and cellular bodies by lymphocytes. *Ductular proliferation stage* (*stage II*) is characterized by small bile ducts proliferation in an attempt to compensate the obstruction of the large bile ducts. The liver characteristically contains few large ducts and many small bile ducts. *Scarring* (*stage III*) is characterized by fibrosis and intrahepatic collagen deposition. *Hepatic cirrhosis* (*stage IV*) is characterized by architectural hepatic disruption and accumulation of the bile within the hepatocytes. The disease is diagnosed by liver biopsy, plus detecting antimitochondrial antibodies (AMA) in the serum.
- *Secondary biliary cirrhosis* arises due to extrahepatic obstruction of the biliary tree, causing bile stagnation within the liver. This type can be seen in cases of congenital bile duct atresia, chronic biliary stone obstruction, or pancreatic head carcinoma. The inflammation in the secondary biliary cirrhosis arises due to secondary infection of the bile, leading to neutrophilic acute inflammatory reaction. In contrast, PBC is a chronic, autoimmune disease with lymphatic and plasma cell inflammatory reaction.
- *Cirrhosis due to metabolic disease* is seen in glycogen storage diseases, α1-antitrypsin deficiency disease, hemochromatosis, and Wilson's disease. All the metabolic cirrhoses are micronodular except Wilson's disease (macronodular).
- *Cirrhosis due to circulatory disorders* is observed in patients with venous congestion due to right-sided heart failure, veno-occlusive disease due to herbal medicine, and Budd–Chiari syndrome. In congestive heart failure, chronic hepatic venous congestion may lead to intrahepatic hypertension, which results in sinusoidal congestion, pressure atrophy, and necrosis of pericentral parenchymal cells. Later, there is a collapse of the necrotic cells with perisinusoidal and periportal collagen deposition (fibrosis) extending to the central veins. These changes are known as "nutmeg liver" on postmortem liver examination.

Cirrhotic nodules are parenchymal nodules found in cirrhotic liver (seen in 25 % of imaging scans only), and they are divided into three main types:

- *Regenerative nodules* represent normal proliferation of liver parenchyma. The development of regenerative nodules can be explained pathologically by cellular repair mechanism known as "cell-to-cell and cell-to-matrix interaction." Cell-to-cell interaction describes the process of cellular inhibition when two cells touch each other (e.g., skin wound healing). Cell-to-matrix interaction describes the process of cellular proliferation inhibition when the regenerated cells touch the tissue matrix (connective tissue frame). In acute hepatitis, if the connective tissue matrix is preserved, then damage to the liver can be completely repaired without architectural distortion or residuals. In contrast, in chronic hepatitis, both the liver parenchyma and the connective tissue frame are damaged. This matrix damage results in random liver cell regeneration without cell-to-matrix cellular inhibition, which will result in regenerative liver nodule formation with fibrosis in between (liver cirrhosis). These nodules do not function normally because the relationship with the portal vein, hepatic artery, and bile ducts (porta hepatis) is lost.
- *Dysplastic nodules* are regenerative premalignant nodules.
- *HCC nodules* are nodules composed of neoplastic cells and are seen commonly in patients with cirrhosis due to hepatitis C virus.

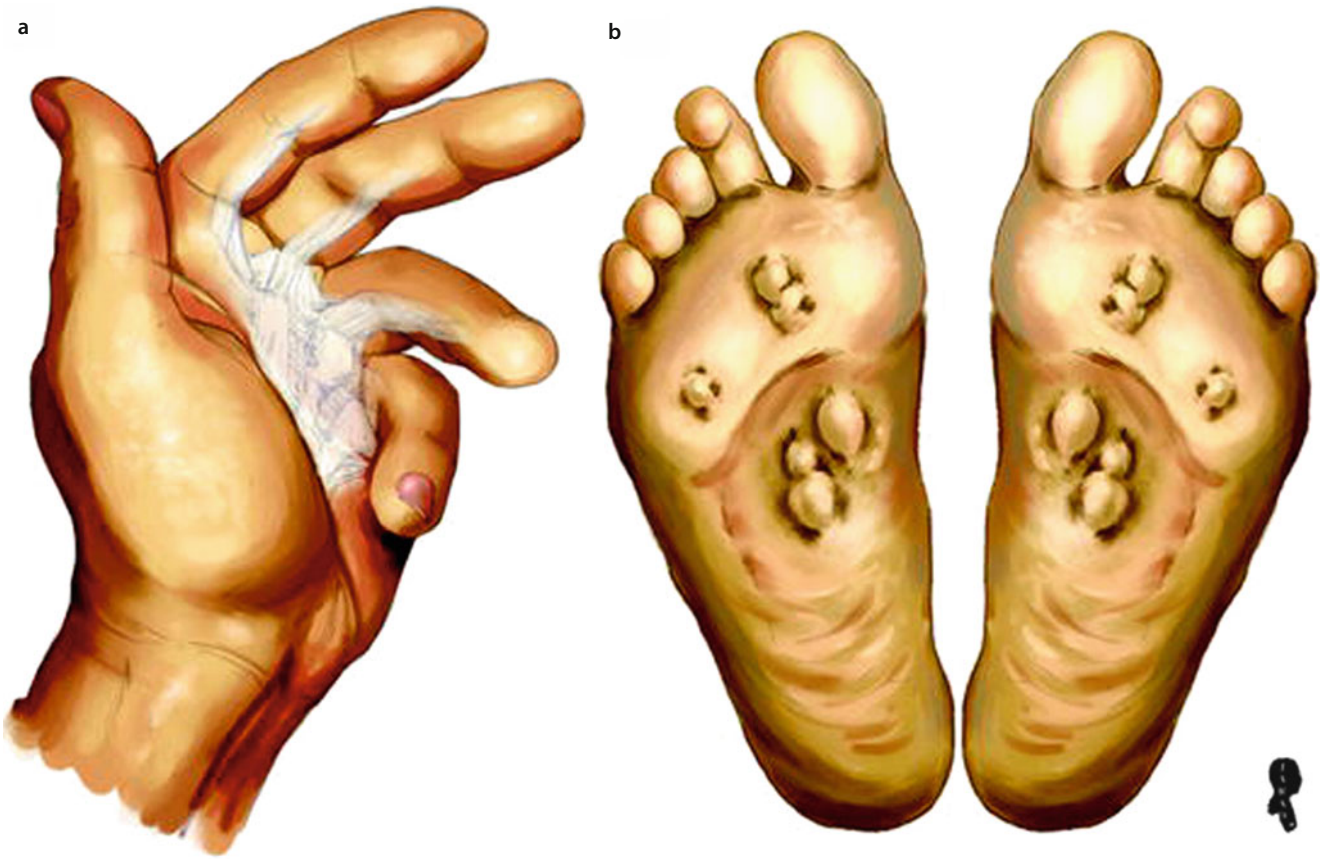

Fig. 1.1.1 An illustration shows the clinical pathological picture of Dupuytren's contracture with illustrated thickening of the palmar aponeurosis (**a**) and bilateral plantar nodules representing the clinical manifestation of Ledderhose disease (**b**)

Patients with cirrhosis are asymptomatic, unless they develop signs of liver failure. Signs of liver failure include yellowish discoloration of the skin (jaundice), development of central arteriole dilatation with radiating vessels on the face (spider nevi), white nail bed due to hypoalbuminemia, painful proliferative arthropathy of long bones, gynecomastia and palmar erythema due to reduced estradiol degeneration by the liver, hypogonadism (mainly in cirrhosis due to alcoholism and hemochromatosis), anorexia and wasting (>50 % of patients), and diabetes mellitus type 2 (up to 30 % of patients). Some patients with liver cirrhosis may develop palmar fibromatosis.

Fibromatosis is a pathological condition characterized by local proliferation of fibroblasts which manifests clinically as soft-tissue thickening. Fibromatosis can affect the palmar aponeurosis (*Dupuytren's contracture*), causing limited hand extension and possibly bony erosions (Fig. 1.1.1). Palmar fibromatosis that occurs in a bilateral fashion and is associated with bilateral plantar fibromatosis is called *Ledderhose disease* (Fig. 1.1.1). Other forms of fibromatosis in the body include the male genital fibromatosis (*Peyronie's disease*) and fibromatosis of the dorsum of the interphalangeal joint (*Garrod's nodes*).

The development of portal hypertension can result in splenomegaly, ascites, and prominent paraumbilical veins (caput medusae). Multiple intra- and extrahepatic portosystemic collaterals develop to compensate the loss of the large portal venous flow that cannot be maintained longer due to increased intrahepatic venous pressure in portal hypertension. Intrahepatic portosystemic shunts occur when the portal vein communicates with the hepatic vein in or on the surface of the liver through a dilated venous system. In contrast, extrahepatic portosystemic shunts occur when the intrahepatic portal vein runs toward the outside of the liver communicating with the systemic veins. *Cruveilhier–Baumgarten syndrome* is a condition characterized by patent paraumbilical vein as a consequence of portal hypertension, which occurs as a part of portosystemic shunts. Paraesophageal and paragastric varices develop in patients with advanced liver cirrhosis and can cause life-threatening upper gastrointestinal (GI) bleeding.

Hepatic encephalopathy is a potentially reversible complication seen in advanced liver failure and cirrhosis characterized by motor, cognitive, and psychiatric central nervous system (CNS) dysfunction. Manifestations of hepatic encephalopathy include daytime deterioration (grade 1), disorientation in space (grade 2), or coma (grade 3).

Flapping tremor (asterixis) may be seen in patients with hepatic encephalopathy. The neurological manifestations of hepatic encephalopathy are due to inability of the liver to detoxify neurotoxins such as ammonia, phenols, short-chained fatty acids, and other toxic metabolites within the blood. These toxic metabolites cross the blood–brain barrier and deposits within the basal ganglia causing encephalopathy. Hepatic encephalopathy can be induced or exaggerated by sedation, high-protein diet, GI hemorrhage, and the use of diuretics.

Hepatopulmonary syndrome is an end-stage liver disease characterized by pulmonary failure, and it is seen in 15–20 % of cirrhosis patients. The diagnosis of hepatopulmonary syndrome requires the following three criteria: chronic liver disease, increased alveolar–arterial gradient on room air, and evidence of intrapulmonary vascular dilatation. Patients with hepatopulmonary syndrome present with liver cirrhosis with hypoxia (30 % of decompensated liver patients). This hypoxemia occurs due to pulmonary vascular dilatation and subsequent ventilation–perfusion mismatch due to decreased hepatic clearance or increased hepatic productions of circulating cytokines and chemical mediators (e.g., nitric oxide). Hypoxic respiratory failure can occur with cases of massive liver necrosis or fulminant hepatic failure.

Hepatitis C virus-related arthritis (*HCVrA*) may be seen in patients with liver cirrhosis due to hepatitis C virus. HCVrA affects 4 % of patients with HCV liver cirrhosis, and it has two forms: a frequent symmetrical polyarthritis affecting small joints similar to rheumatoid arthritis in a lesser form and an intermittent mono-/oligoarthritis that involves medium- and large-sized joints.

Signs on Plain Radiographs

- *Hepatic hydrothorax* is defined as large pleural effusion in a cirrhotic liver disease patient in the absence of cardiac or pulmonary disease. Hepatic hydrothorax is seen in 10 % of patients. The pleural effusion can be right sided (67 %), left sided (17 %), or bilateral (17 %).
- Hepatopulmonary syndrome is visualized on plain chest radiographs as reticulonodular interstitial pattern located mainly at the lung bases (46–100 % of cases).
- Noncardiogenic pulmonary edema can be seen in 37 % in patients with fulminant hepatic failure.
- Esophageal varices may manifest on chest radiographs as focal lateral displacement of the mediastinum.
- On abdominal radiographs, ascites is detected as loss of the abdominal gases and the normal psoas shadows visualization. The abdomen structures are blurry due to the overlying fluid shadow (Fig. 1.1.2).

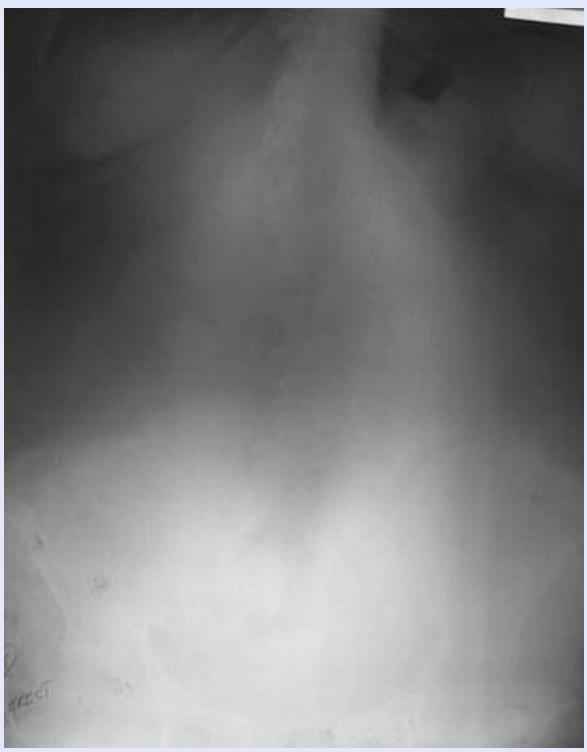

Fig. 1.1.2 Plain abdominal radiograph in a patient with massive ascites shows complete blurry abdomen

Signs on US

- Cirrhosis is detected as irregular nodular liver contour with inhomogeneous echo-texture. Liver right lobe atrophy with enlarged caudate lobe is a typical finding (caudate lobe/right lobe ratio >0.65) (Figs. 1.1.3 and 1.1.4).
- Mixed hypoechoic and hyperechoic texture of the liver parenchyma is detected when regenerative nodules are found.
- Signs of portal hypertension include splenomegaly (>12 cm), ascites, and dilated venous collaterals.

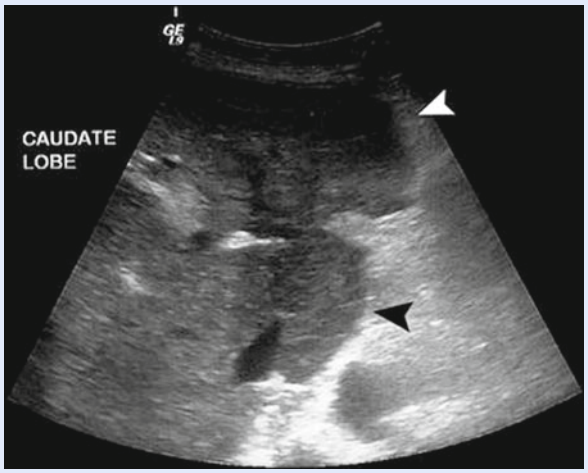

Fig. 1.1.3 Transverse ultrasound image of a patient with liver cirrhosis shows atrophied left lobe (*white arrowhead*), with hypertrophied caudate lobe (*black arrowhead*)

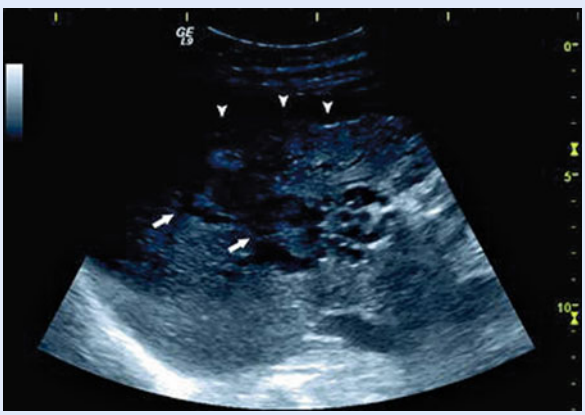

Fig. 1.1.4 Transverse ultrasound image of a patient with liver cirrhosis due to hepatitis C virus shows irregular liver contour (*arrowheads*), with two intrahepatic liver hypoechoic masses, which were diagnosed on liver triphasic CT scan later as hepatocellular carcinoma (HCC) masses (*arrows*)

Signs on Doppler Sonography

- *Hepatic veins*: hepatic veins join immediately the inferior vena cava, which is in direct communication with the left atrium. Due to the previous anatomical fact, the normal hepatic veins waveform is "triphasic," because it is affected by left atrial cardiac motion and Valsalva maneuver (Fig. 1.1.5). In patients with cirrhosis, the triphasic flow pattern is converted into biphasic and monophasic depending on the severity of cirrhosis.
- *Portal vein*: it supplies 70–80 % of the incoming blood to the liver, and the hepatic artery supplies only 20–30 %. The normal portal venous flow is always toward the liver (hepatopetal). The fasting mean velocity of normal portal vein is approximately 18 cm/s (range, 13–23 cm/s[3]), and the flow pattern is normally flat or monophasic (Fig. 1.1.6). Mildly pulsatile portal venous flow pattern can be seen normally in tall, thin patients (Fig. 1.1.7). Portal hypertension is detected as hepatic blood flow away from the liver (hepatofugal) due to increased intrahepatic venous flow resistance. Portal vein diameter (>13 mm) and splenic vein diameter (>10 mm) are other signs of portal hypertension. Hepatic vein thrombosis can be seen in patients with HCC, and it is visualized as partial or complete loss of flow signal within the portal vein.
- *Hepatic artery*: the normal hepatic artery in a fasting patient has a systolic velocity of approximately 30–40 cm/s and a diastolic velocity of 10–15 cm/s. The flow pattern normally is monophasic and has low resistance, with high diastolic flow (Fig. 1.1.8). The resistance index (RI), which is defined as the maximal systolic velocity minus the end-diastolic velocity divided by the maximal velocity, varies normally in a fasting patient from 0.55 to 0.81. There is increase in hepatic artery RI after mean or with age in a healthy person. The hepatic artery diastolic velocity is less than the peak portal vein velocity, and if the hepatic diastolic velocity is greater than the portal vein, one should suspect hepatic parenchymal disease. Also, the RI increases in patients with cirrhosis, and the after meal variation is absent (Fig. 1.1.9).
- *Cruveilhier–Baumgarten syndrome* is detected as a patent vein located at the umbilicus with typical monophasic venous flow (Fig. 1.1.10). The vein can be followed by the probe until identifying its relation to the intrahepatic portal veins passing through the ligamentum teres (Fig. 1.1.11).

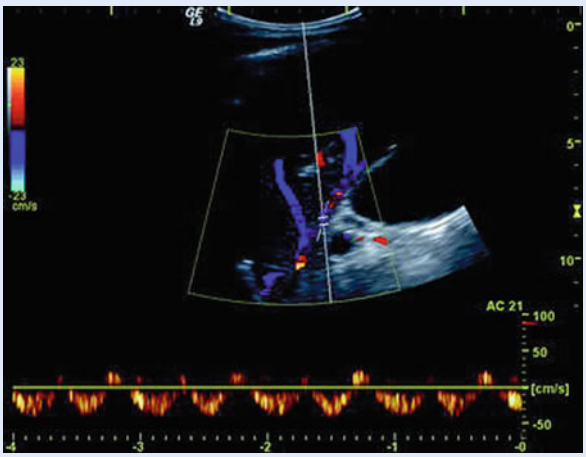

Fig. 1.1.5 Color Doppler waveform spectrum of the hepatic veins shows the normal venous triphasic pattern

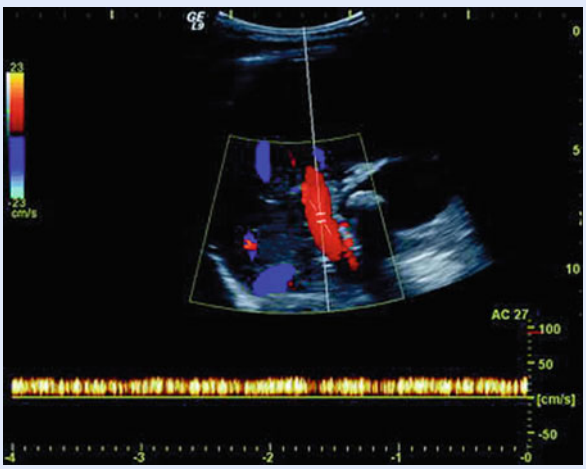

Fig. 1.1.6 Color Doppler waveform spectrum of the portal vein shows the normal monophasic pattern

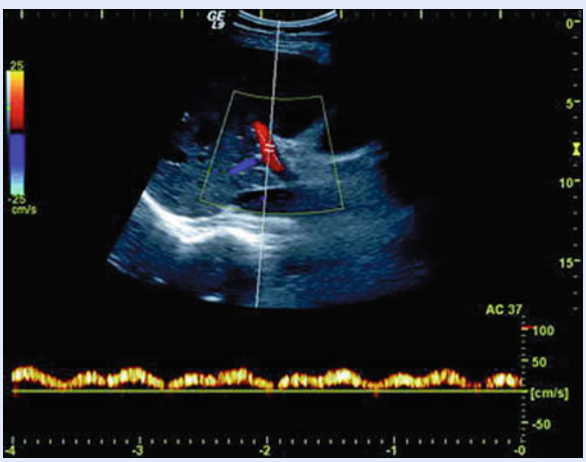

Fig. 1.1.7 Color Doppler waveform spectrum of the portal vein shows the physiologic portal vein pulsation in athletic tall patient who came for a routine abdominal ultrasound checkup

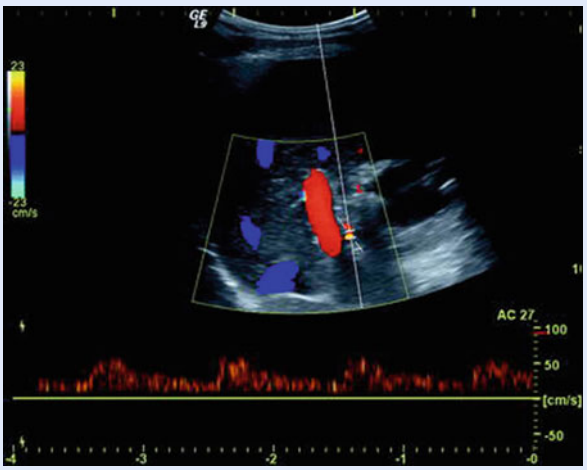

Fig. 1.1.8 Color Doppler waveform spectrum of the hepatic artery shows the normal monophasic, low-resistance with high diastolic flow arterial pattern

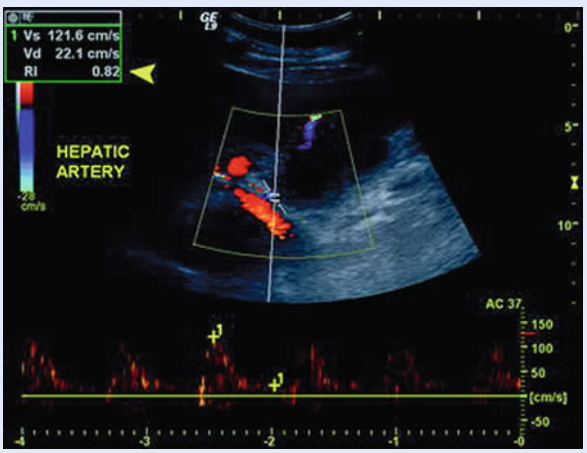

Fig. 1.1.9 Hepatic artery color Doppler waveform spectrum in a patient with alcoholic liver cirrhosis shows high RI (*arrowhead*)

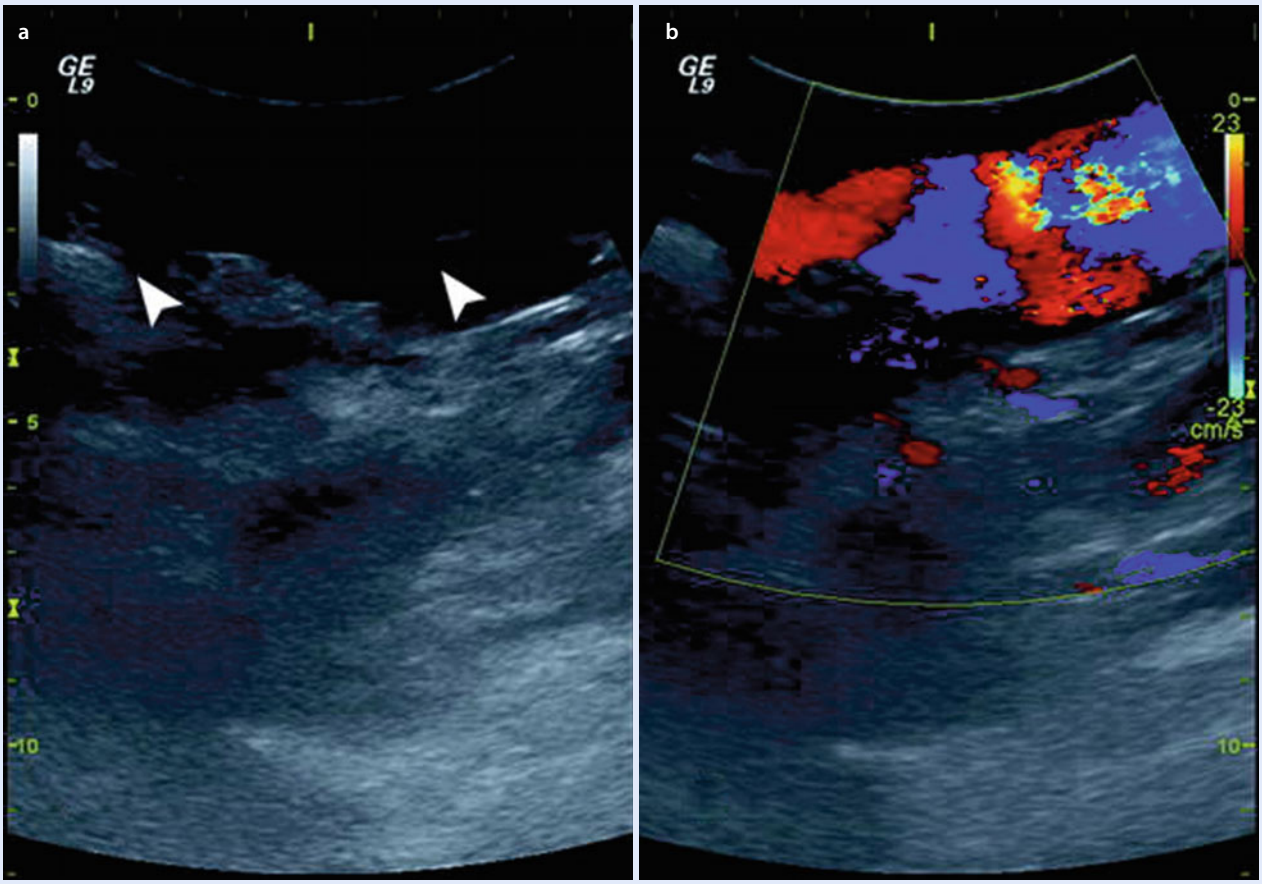

Fig. 1.1.10 Color Doppler sonography image shows patent umbilical vein at the level of the umbilicus (*arrowheads*) in a patient with chronic liver cirrhosis and Cruveilhier–Baumgarten syndrome

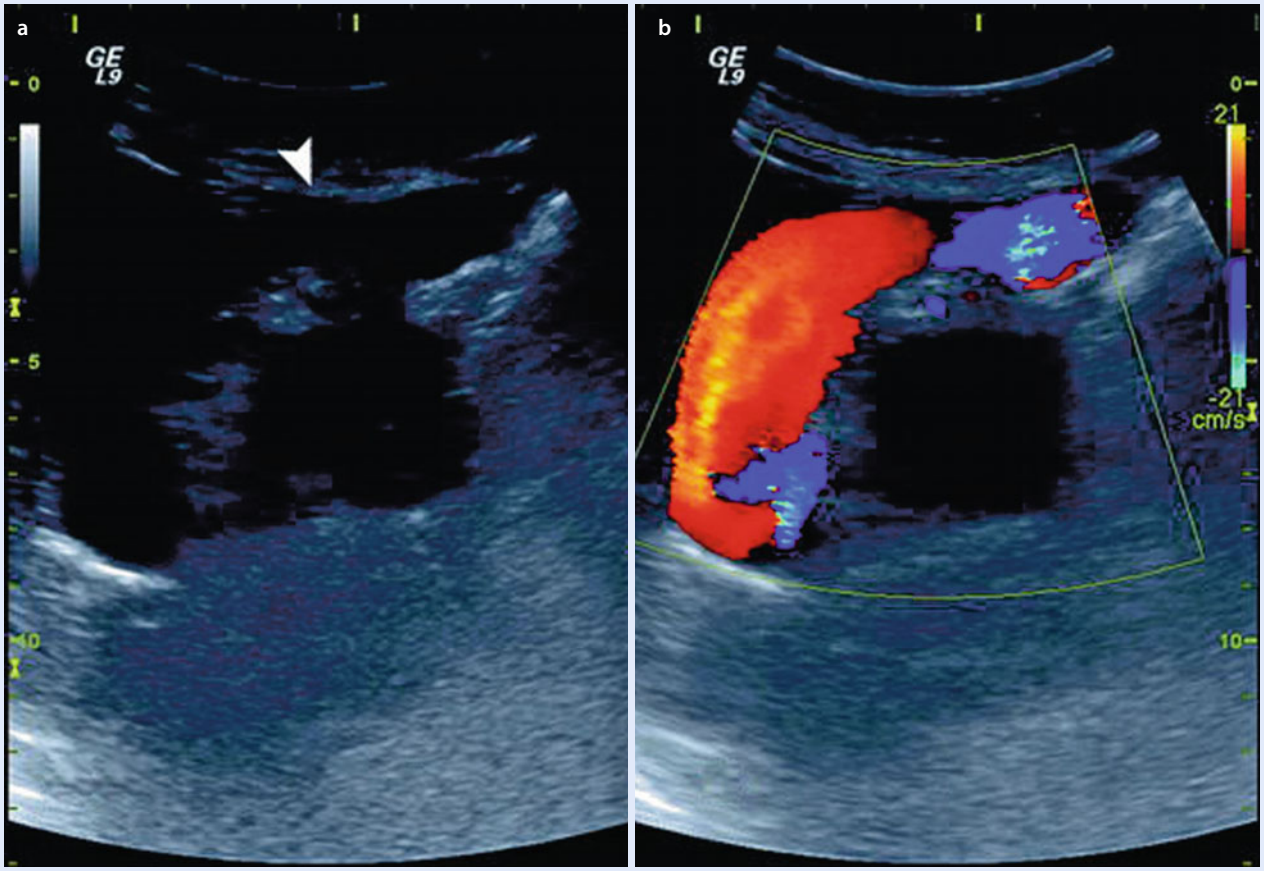

Fig. 1.1.11 The same patient shows the connection of the patent umbilical vein to the dilated portal vein through the ligamentum teres (*arrowhead*)

Signs on Barium Swallow

- Esophageal varices are visualized as serpiginous filling defects in the esophagus, usually located in the lower third (Fig. 1.1.12).

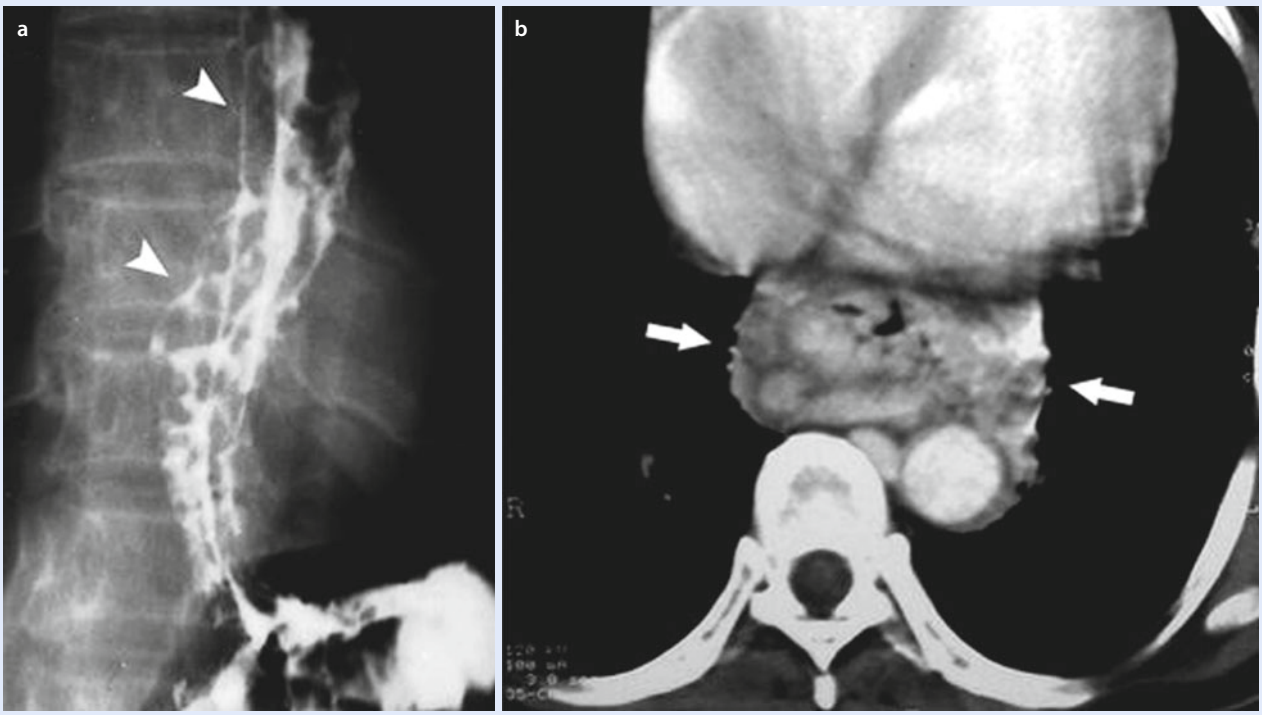

Fig. 1.1.12 Barium swallow (**a**) and axial thoracic-enhanced CT (**b**) images in two patients with esophageal varices. In (**a**), the varices are visualized as serpiginous filling defects in the lower esophagus (*arrowheads*). In (**b**), esophageal varices are visualized as multiple paraesophageal enhanced tubular densities adjacent to the esophageal wall (*arrows*)

Signs on CT

- Cirrhotic liver appears small (<15 cm), with atrophied right lobe and enlarged caudate and left lobes. The liver contour is nodular and irregular due to parenchymal atrophy and nodular regeneration (Fig. 1.1.13).
- *Regenerative nodules* are divided into micronodules (<3 mm in diameter) and macronodules (>3 mm in diameter). They do not enhance in arterial phase because they are supplied mainly by portal vein and enhance like a normal liver parenchyma. Occasionally, they may accumulate iron within them, which will make them seen in noncontrast scans as hyperdense nodules (*siderotic nodules*), which are typically seen in alcoholic liver cirrhosis.
- *Dysplastic nodules* are siderotic nodules larger than 1 cm. They enhance homogeneously in both arterial and portal phases and are usually not seen in scans. Few nodules may show enhancement in the arterial phase and only differentiated from HCC by biopsy.
- *Hepatocellular nodule* is seen as a hypodense area in nonenhanced CT scan and shows enhancement in the arterial phase, which is the key to HCC diagnosis. Up to 50 % of nodules are not detected in the arterial phase because they behave as a normal liver parenchyma in the triphasic hepatic scan. The nodules become hypodense again in the portal venous phase of the scan (Fig. 1.1.13).
- *Portal hypertension* can be detected if the portal vein diameter increases (>13 mm). Also, splenomegaly, dilated perisplenic collateral venous channels, and ascites may be found as signs of portal hypertension (Fig. 1.1.14).
- *Esophageal varices* are seen as multiple, enhanced nodular or tubular densities inside the esophageal lumen (intraluminal varices) or adjacent to the esophageal wall (paraesophageal varices) (Fig. 1.1.12).

- Enlarged porta hepatic lymph nodes might be seen in end-stage cirrhotic liver.
- *Cruveilhier–Baumgarten syndrome* is visualized as an abnormal vein that arises from the right or left intrahepatic portal vein and leaves the liver via ligamentum teres to attach itself to the umbilicus on the portal phase of contrast-enhanced liver CT (Fig. 1.1.15).
- On chest HRCT, *hepatopulmonary syndrome* is visualized as peripheral pulmonary arteriole dilatation with increased numbers of terminal branches extending to the pleura (Fig. 1.1.16).
- Liver venous hypertension due to congestive heart failure (nutmeg liver) may show characteristic reticulo-mosaic pattern of enhancement on postcontrast examinations (Fig. 1.1.17).

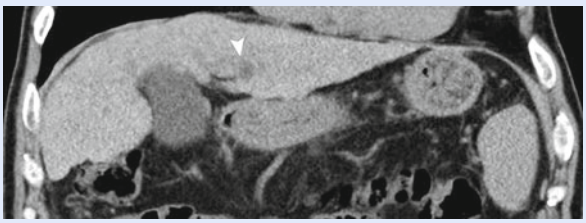

Fig. 1.1.13 Coronal nonenhanced CT image shows mildly shrunken liver due to cirrhosis with mild irregular contour and hypodense nodule in segment IVb (*arrowhead*), which was proven later to be HCC

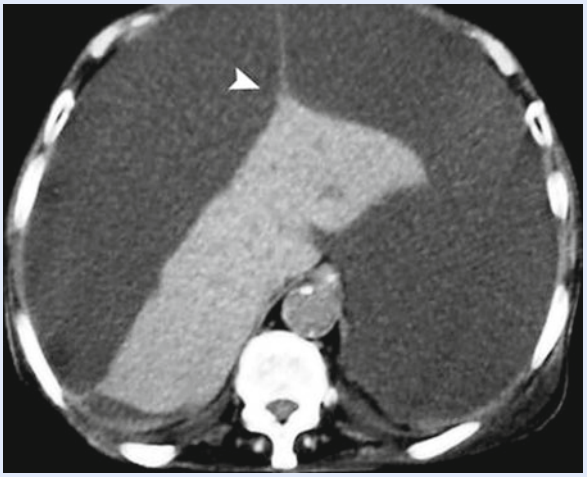

Fig. 1.1.14 Axial CT scan in a patient with liver cirrhosis shows massive ascites that nicely demonstrates ligamentum teres (*arrowhead*)

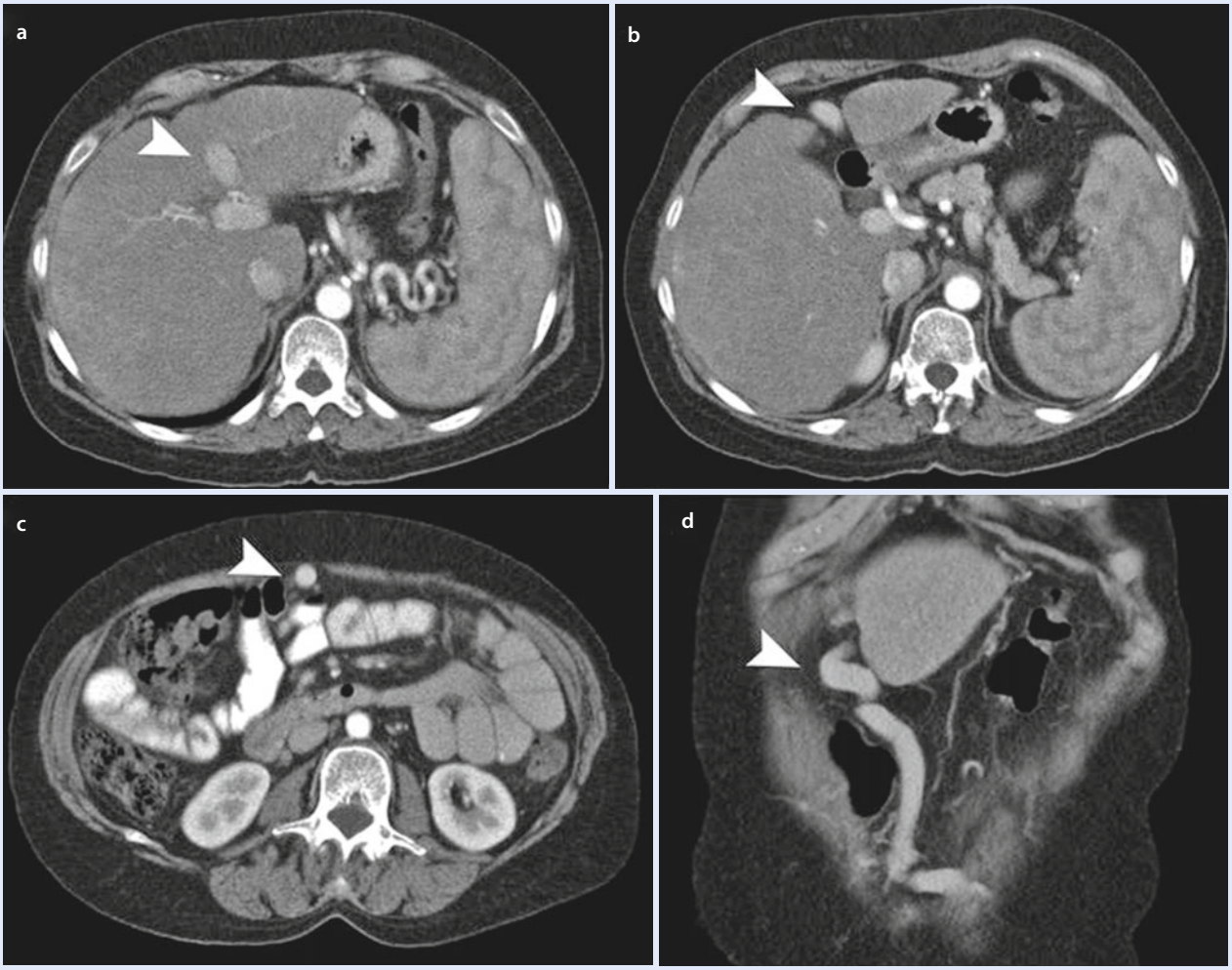

Fig. 1.1.15 Sequential axial abdominal enhanced CT of a patient with liver cirrhosis shows patent umbilical vein arises from the left portal vein (**a**), runs through ligamentum teres (**b**), and joins the umbilicus (**c**). The course of the patent vein can be seen in the coronal image in (**d**)

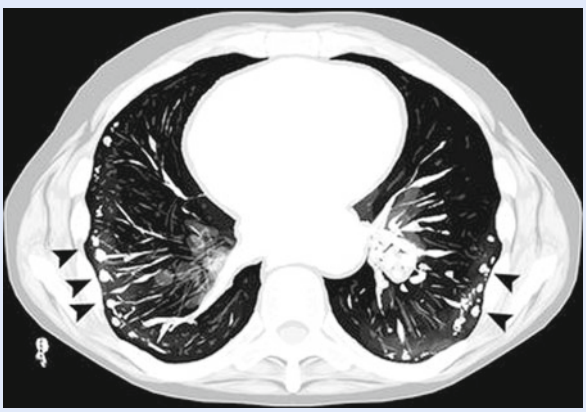

Fig. 1.1.16 Axial chest HRCT illustration shows multiple dilated peripheral pulmonary arterioles demonstrating hepatopulmonary syndrome in patients with liver cirrhosis

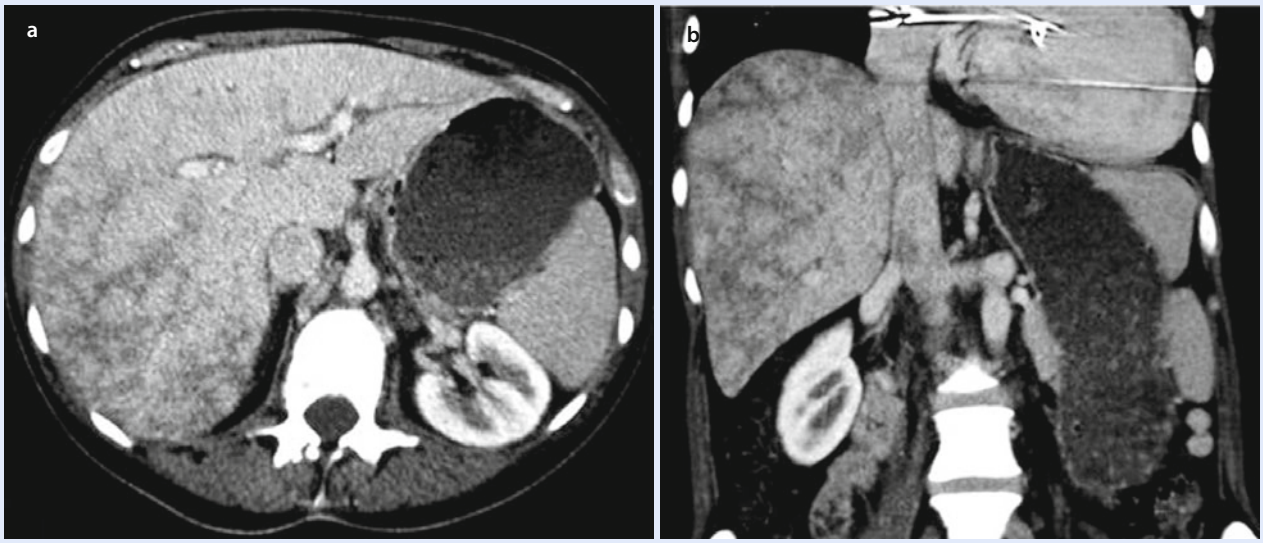

Fig. 1.1.17 Axial (**a**) and coronal (**b**) contrast-enhanced CT in a patient with right-sided heart failure due to tricuspid regurgitation shows the characteristic reticulo-mosaic pattern of enhancement of hepatic venous congestion

Signs on MRI

- *Hepatic encephalopathy* has bilateral and symmetrical high-intensity signal on T1W images in the basal ganglia, especially in the globus pallidus (Fig. 1.1.18). The extent of the basal ganglia disease is related to the plasma level of ammonia. Cerebellar atrophy may be seen in advanced stages.
- Regenerated nodules with or without hemosiderin have low T2 signal intensity. In contrast, a hepatic carcinoma nodule appears hyperintense on T2W images and shows early arterial-phase contrast enhancement.
- In *PBC*, periportal hyperintensity signal on T2W images is observed in the initial stages of the disease (stages I and II), reflecting active periportal inflammation (Fig. 1.1.19). A *periorbital halo sign* may be seen as low-intensity signal centered around the portal venous branches on T2W images (Fig. 1.1.19). This sign is specific for the diagnosis of PBC. Lastly, a peripheral small wedge-shaped area may be seen in the early phases of liver contrast study, which represents arterial–portal shunting.
- Up to 50 % of uncompensated cirrhotic patients show dilated cisterna chyli, which is seen as high T2 signal intensity structure adjacent to the aorta, with delayed enhancement several minutes after gadolinium injection. This sign is detected on CT in 1.7 % of uncompensated cirrhotic patients.
- Plantar fibromatosis is visualized as bilateral infiltrative masses located at the deep aponeurosis adjacent to the plantar muscles in the medial aspect of the foot (Fig. 1.1.20). The masses typically show low T1 and T2 signal intensities due to the fibrous nature of the lesion. After contrast injection, enhancement of the masses can be seen in approximately 50 % of cases.

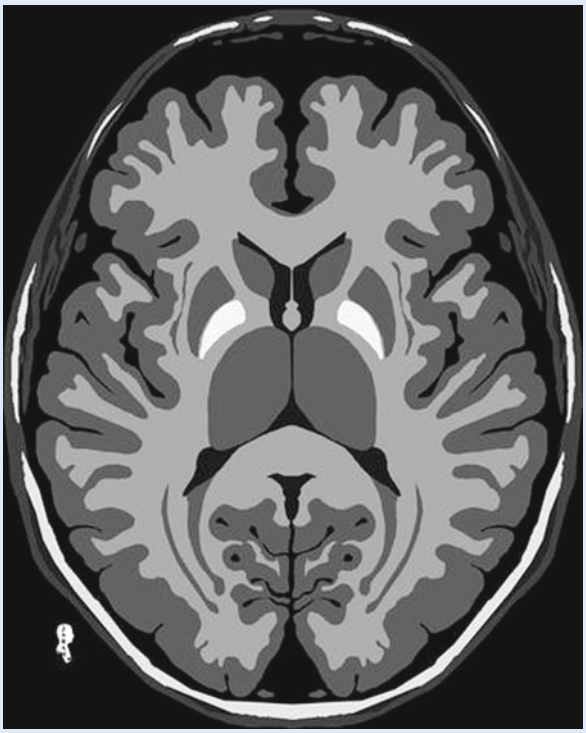

Fig. 1.1.18 Axial T1W MR illustration shows bilateral symmetrical high density in the globus pallidus representing sign of hepatic encephalopathy

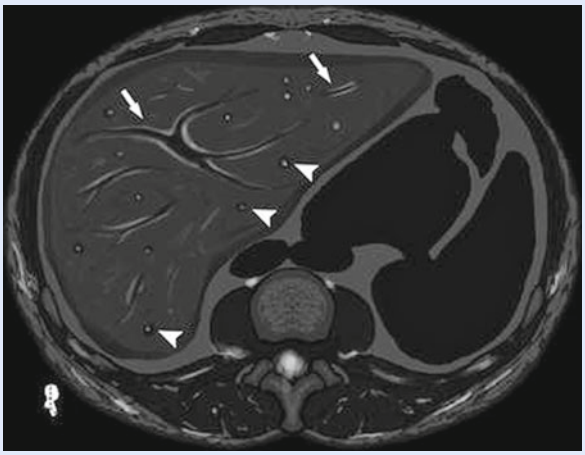

Fig. 1.1.19 Axial T2W MR illustration of the liver demonstrates the periportal hyperintensity (*arrows*) and the periorbital halo sign (*arrowheads*)

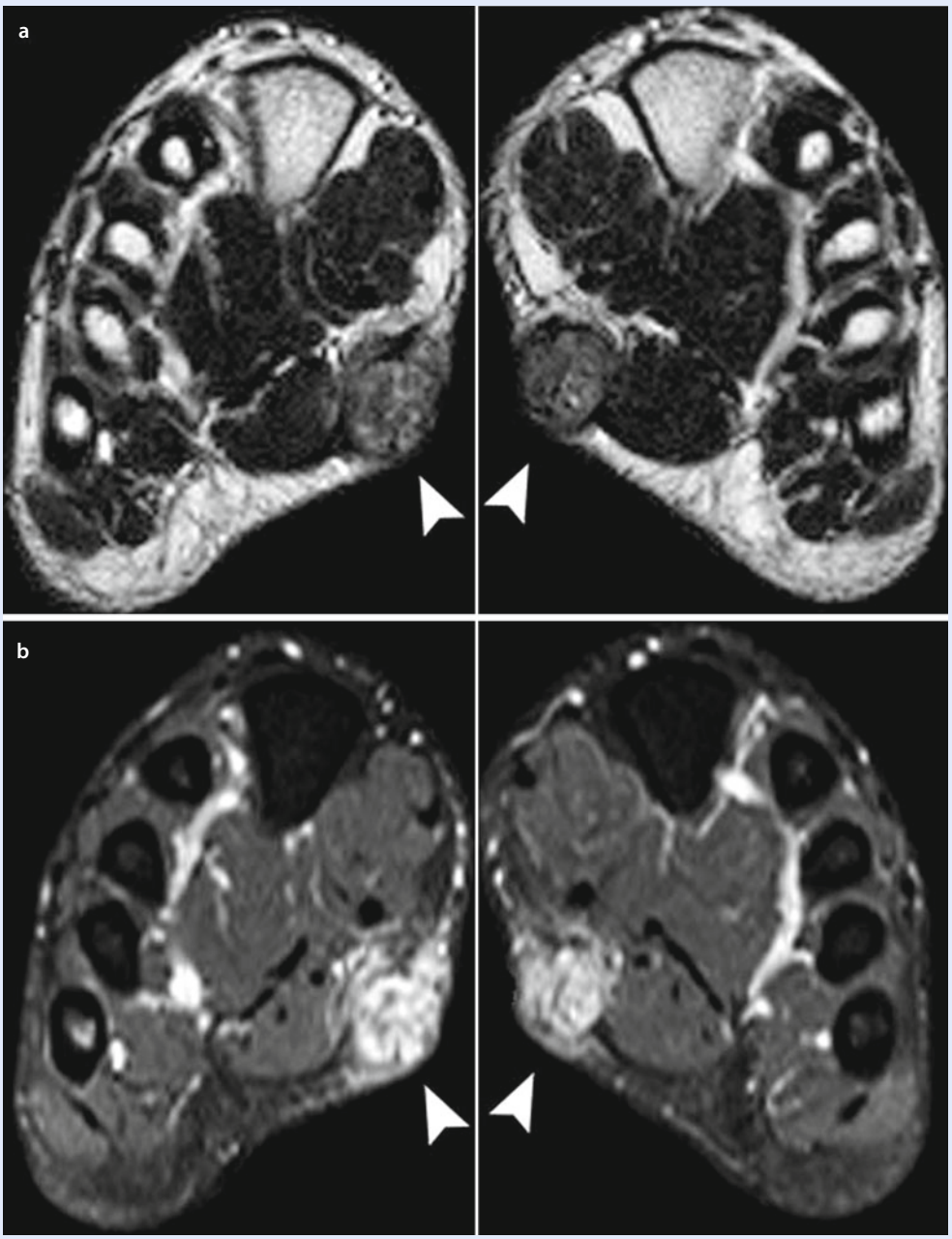

Fig. 1.1.20 Axial-oblique T2W (**a**) and T1W postcontrast MRI of the feet shows bilateral hypointense plantal masses (*arrowheads*) on image (**a**) diagnostic of Ledderhose disease (plantar fibromatosis). The masses show marked contrast enhancement after gadolinium injection (**b**)

Further Reading

Ba-Ssalamah A, et al. Dedicated multi-detector CT of the esophagus: spectrum of diseases. Abdom Imaging. 2009; 34:3–18.

Bonekamp S, et al. Can imaging modalities diagnose and stage hepatic fibrosis and cirrhosis accurately? J Hepatol. 2009;50:17–35.

Chavhan GB, et al. Normal Doppler spectral-waves of major pediatric vessels: specific patterns. Radiographics. 2008; 28:691–706.

Colli A, et al. Severe liver fibrosis or cirrhosis: accuracy of US for detection – analysis of 300 cases. Radiology. 2003;227:89–94.

Ito K, et al. Imaging findings of unusual intra- and extrahepatic portosystemic collaterals. Clin Radiol. 2009;64:200–7.

Kobayashi S, et al. MRI findings of primary biliary cirrhosis: correlation with Scheuer histologic staging. Abdom Imaging. 2005;30:71–6.

Lim JH, et al. Regenerative nodules in liver cirrhosis: findings at CT during arterial portography and CT arteriography

with histopathologic correlation. Radiology. 1999;210: 451–8.
Martinez-Noguera A, et al. Doppler in hepatic cirrhosis and chronic hepatitis. Semin Ultrasound CT MR. 2002;23:19–36.
Mauro MA, et al. Computed tomography of hepatic venous hypertension: the reticulated – mosaic pattern. Gastrointest Radiol. 1990;15:35–8.
Meyer CA, et al. Diseases of the hepatopulmonary axis. Radiographics. 2000;20:687–98.
Palazzi C, et al. Hepatitis C virus-related arthritis. Autoimmun Rev. 2008;8:48–51.
Schuppan D, et al. Liver cirrhosis. Lancet. 2008;371:838–51.
Sharma S, et al. MRI diagnosis of plantar fibromatosis – a rare anatomic location. Foot. 2003;13:219–22.
Verma SK, et al. Dilated cisternae chyli: a sign of uncompensated cirrhosis at MR imaging. Abdom Imaging. 2009;34: 211–6.

1.2 Fatty Liver Disease (Liver Steatosis)

Accumulation of lipid within cells is a pathologic process. Any type of lipid can accumulate within cells, such as cholesterol, triglycerides, and phospholipids. Fatty liver disease (steatosis) is characterized by accumulation of triglycerides within hepatocytes.

Normally, free fatty acids are taken up by the hepatocytes and then converted into cholesterol esters, triglycerides, ketone bodies, or phospholipids. Some of the lipids combine with apoproteins to form a specific type of lipoprotein called very-low-density lipoprotein (VLDL), which is then secreted into the blood. Liver steatosis can result from either excess delivery of free fatty acids into the liver (e.g., diabetes mellitus), increased formation of lipids within the liver (e.g., alcohol ingestion), hepatocytes disease (e.g., hepatitis), or decreased formation of VLDL by the liver (e.g., protein malnutrition).

Types of Liver Steatosis

- *Diffuse fatty infiltration*: the liver is usually enlarged with uniform decrease in density in the liver scan.
- *Focal fatty infiltration*: there is an area of the liver that shows fatty infiltration while the rest of the liver is normal. It usually occurs in the same areas that are supplied by the third inflow systemic veins (porta hepatic, around ligamentum teres, and adjacent to gallbladder). It is seen most commonly in the left lobe of the liver.
- *Multiple fatty infiltrations*: there are scattered low-density areas within a normal density liver. This type can be easily mistaken with metastases on noncontrast-enhanced liver CT scan.
- *Focal sparring*: there are areas of normal liver parenchyma surrounded by large areas of low-density diffuse fatty infiltration. This type also may simulate neoplasms on noncontrast-enhanced liver CT scan.

Signs on US

- Fatty liver is visualized as highly echogenic liver. The high liver echogenicity can be compared to the echogenicity of the right renal cortex, which will show marked difference in echogenicity (Fig. 1.2.1).
- Focal fatty infiltration is seen as a focal, highly echogenic area within a relatively isoechoic (normal) liver parenchyma (Fig. 1.2.2).
- Focal sparring is seen as a focal area which is relatively hypoechoic (normal) within a highly echogenic liver.

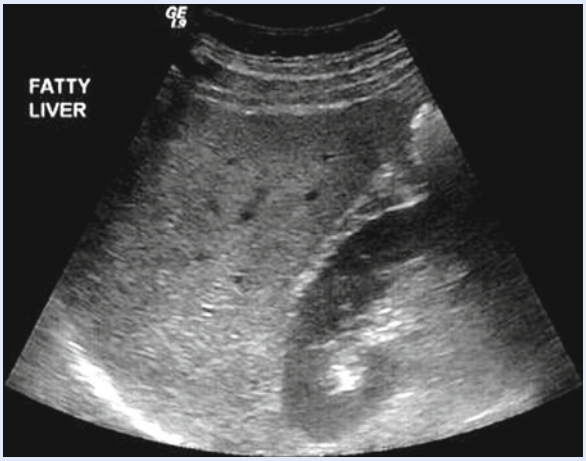

Fig. 1.2.1 Transverse ultrasound image of the liver shows diffuse increase in liver echogenicity compared to the right renal cortex (liver steatosis)

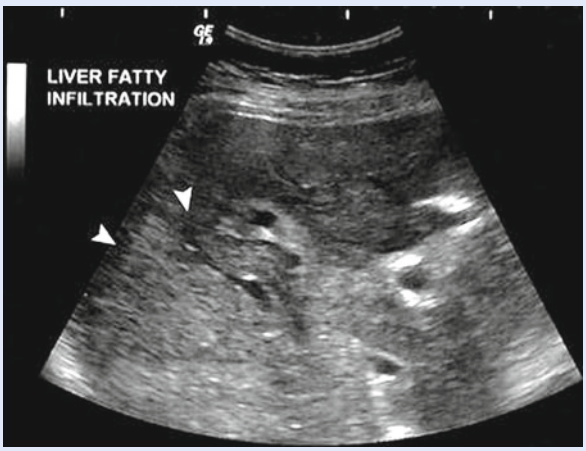

Fig. 1.2.2 Transverse ultrasound image of the liver shows focal fatty infiltration involving segment VI and segment VII

Signs on CT

- Hepatic steatosis is detected as diffuse or focal reduction of the liver normal density on noncontrast-enhanced scan (Fig. 1.2.3). The normal liver density is 8 HU (Hounsfield unit) above that of the spleen (60 HU). Fatty liver density is 10 HU below spleen density on noncontrast-enhanced scan (if the normal spleen is 52 HU, then the fatty liver is <42 HU).
- Focal fatty infiltration is seen as a hypodense area with nonspherical margins (metastases usually have round edge). The hypodense area or the mass does not show mass effect over the parenchyma around it and shows change over time (seen in films before the current scan or after few months' scan). The same criteria are applied to the focal sparring, but the mass will be isodense within a hypodense liver on noncontrast-enhanced scan.
- In both focal sparring and focal fatty infiltration, hepatic vessels course within the fatty infiltration or focal sparring undisturbed. In contrast, metastases or other hepatic lesions will be cutting off the hepatic vessels when they reach them.

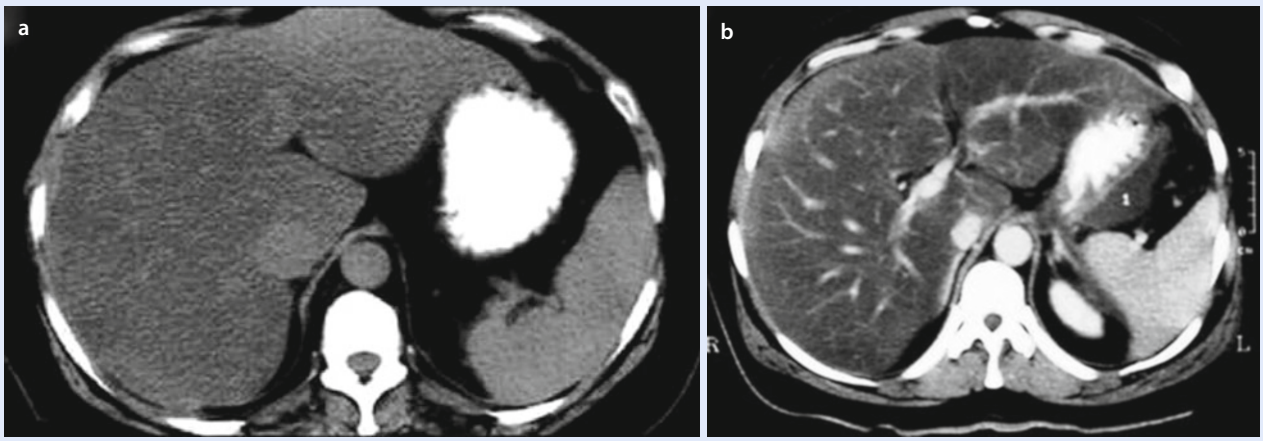

Fig. 1.2.3 Axial precontrast (**a**) and postcontrast (**b**) abdominal CT images show diffuse hepatic steatosis. Notice the density of the liver compared to the spleen in pre- and postcontrast images

Signs on MRI

- Liver steatosis is diagnosed on MRI when the liver intensity drops to >30 % difference on both T1W in-phase and T1W out-of-phase images (Fig. 1.2.4).

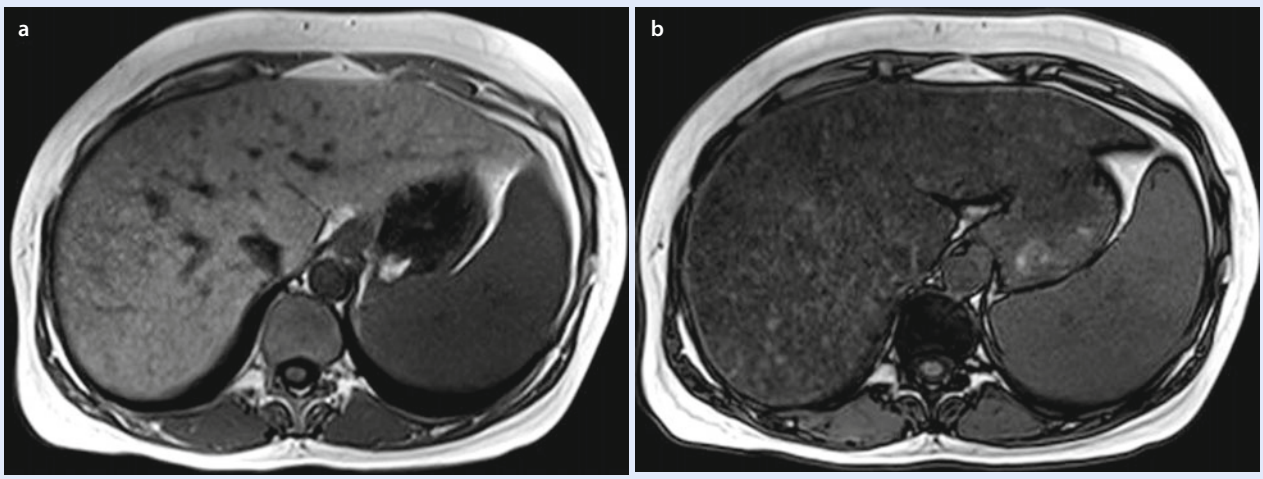

Fig. 1.2.4 Axial T1W in-phase (**a**) and T1W out-of-phase (**b**) MRI in a patient with liver steatosis shows drop in the liver signal intensity >44 % in the T1W out-of-phase image (**b**), diagnostic of hepatic steatosis

Further Reading

Alpern MB, et al. Focal hepatic masses and fatty infiltration detected by enhanced dynamic CT. Radiology. 1986;158: 45–9.

Cassidy FH, et al. Fatty liver disease: MR imaging techniques for the detection and quantification of liver steatosis. Radiographics. 2009;29:231–60.

Karcaaltincaba M, et al. Imaging of hepatic steatosis and fatty sparing. Eur J Radiol. 2007;61:33–43.

Sabir N, et al. Correlation of abdominal fat accumulation and liver steatosis: Importance of ultrasonographic and anthropometric measurements. Eur J Ultrasound. 2001; 14:121–8.

Salmonson EC, et al. Focal periportal liver steatosis. Abdom Imaging. 1993;18:39–41.

Yates CH, et al. Focal fatty infiltration of the liver simulating metastatic disease. Radiology. 1986;159:83–4.

1.3 Recurrent Epigastric Pain

Epigastric pain is a term used to describe dull achy pain located at the area of the epigastrium beneath the xyphoid process. Epigastric pain is a very common complaint encountered in both medical and surgical casualty departments. Diagnosis often is established by proper history, examination, and laboratory investigations. This topic discusses some causes of recurrent epigastric pain, in which radiology can play an important role in establishing the underlying diagnosis.

Gastroesophageal Reflux Disease

Gastroesophageal reflux disease (GERD) is a disease characterized by reduction of the lower esophageal sphincter pressure resulting in leaking of the stomach acidity into the lower third of the esophagus, causing esophagitis and epigastric pain.

The most common cause of GERD is hiatus hernia. Four types of hiatus hernias are known: sliding, paraesophageal, sliding and paraesophageal, and complete stomach herniation into the thorax.

Patients with GERD typically present with long-standing mild to moderate epigastric pain with burning sensation, usually postprandial. Severe cases of GERD may manifest due to propagation of gastric acidity to the upper esophagus. Symptoms like aspiration pneumonia, laryngitis, and teeth decay may be seen uncommonly due to advanced GERD. Medical treatments include antacids, histamine (H2) blockers, and proton pump inhibitors. Surgical management with gastric fundoplication is usually advised in cases where the medical therapy fails to control the symptoms.

Barium swallow is the most sensitive method to detect GERD and esophagitis. Esophagitis is defined as defects in the esophageal mucosa due to exposure to the gastric reflux acid and pepsin. *Barrett's esophagus* (BS) is a condition characterized by esophageal mucosal healing in a persistent acid environment. This healing process is characterized by metaplasia of the normal esophageal stratified squamous epithelium into columnar, gastric-like epithelium. Metaplasia is transformation of one cell type to another (e.g., cuboidal cell to columnar cell). BS has the potential for neoplastic transformation. Up to 50 % of patients with GERD show esophageal dysmotility disorders (EDM).

On barium swallow, sliding hiatus hernia is detected by identifying Schatzki ring. An esophageal ring is a short annular narrowing of the esophagus <1 cm in diameter. *Esophageal A ring* is a ring made up of smooth muscles that is seen at the tubulovestibular junction (muscular ring). *Esophageal B ring* (*Schatzki ring*) is an esophageal ring that is only visible radiologically when there is sliding hiatus hernia and is caused by propagation of the gastroesophageal junction above the diaphragm. *Esophageal C ring* is the normal abdominal retroperitoneal esophageal part (3 cm long) which makes a groove on the liver. In contrast to esophageal ring, *esophageal stricture* is defined as an esophageal segment with fixed narrowing. *Esophageal web* is an abnormal thick 1–2 mm diaphragm-like membrane that extends partially or completely around the esophageal lumen and always indents the esophagus anteriorly. The lower esophageal sphincter line where mucosal change is observed between the esophagus and the stomach on barium examination is sometimes referred to as the *Z-line*.

Esophageal dysmotility disorders are a group of diseases characterized by abnormal esophageal peristalsis seen on barium swallow. Types of EDM are tertiary contractions, corkscrew esophagus, esophageal achalasia, esophageal chalasia, and presbyesophagus.

Tertiary esophageal contraction is a nonpulsatile, uncoordinating contraction of the esophageal circular smooth muscles. The normal primary and secondary contractions of the esophagus help to push the food and fluids through the esophagus. This type of dysmotility is often seen with old age or GERD. *Corkscrew esophagus* is a term used to describe the same dysmotility as in tertiary contractions but arises posterior to the heart, causing pain in the retrocardiac region during swallowing. *Esophageal achalasia* is a disease characterized by contraction and narrowing of the esophagus due to a defect in the normal neuronal plexuses within the esophageal muscles, which results in failure of the smooth muscles to relax when the food arrives. Achalasia is commonly seen in the lower third of the esophagus. Achalasia can occur without prior cause (primary) or due to underlying pathology like Chagas' disease or malignancy (secondary). *Esophageal chalasia* is characterized by dilatation and widening of the gastroesophageal junction. *Presbyesophagus* is an asymptomatic condition characterized by failure of the primary peristaltic wave to pass completely through the esophagus, resulting in a combination of tertiary contractions, aperistalsis, and failure of the lower esophageal sphincter to contract (curling phenomenon).

Hiatus hernia can be congenitally seen in neonates and children. The most common congenital hiatal hernias are

Morgagni and Bochdalek's hernias. *Morgagni hernia* is stomach or bowel herniation into the thorax due to diaphragmatic defects that occurs in the anterior/inferior mediastinum. *Bochdalek's hernia* is stomach or bowel hernia into the thorax due to diaphragmatic defects that occurs in the inferior/posterior mediastinum.

Differential Diagnoses and Related Diseases

- *Steakhouse syndrome* is a term used to describe acute food impaction of the esophagus, usually at its distal third. The most common cause of food impaction is esophageal webs. Patients often present to the emergency ward with acute esophageal food impaction, especially after meat ingestion, where the name came from. Patients present with intense retrosternal pain, which may be cardiac in origin, especially if the impacted food presses over the posterior cardiac border. Plain chest radiographs should be performed to exclude bony material impaction or signs of pulmonary aspiration.
- *Plummer–Vinson syndrome* (*Paterson–Kelly syndrome*) is a disease characterized by dysphagia, iron-deficiency anemia, and esophageal webs. Patients are commonly women (85 %), between 30 and 70 years of age. Upper aerodigestive tract carcinoma is seen in 4–16 % of cases, with almost all cases occurring at the postcricoid location.

Signs on Chest Radiographs

- Hiatal hernia is diagnosed by finding the stomach bubble within the thorax, rather than under the left hemidiaphragm (Fig. 1.3.1).
- Morgagni hernia is demonstrated as a mass, bowel loop, or stomach bubble lying in the inferior/anterior mediastinum on lateral radiographs (Fig. 1.3.2). In contrast, Bochdalek's hernia is demonstrated as mass, bowel loop, or stomach bubble lying in the inferior/posterior mediastinum on lateral radiographs (Fig. 1.3.3).
- In esophageal achalasia, there is paramediastinal shadow (widening of the mediastinum), with air–fluid level seen in the retrocardiac shadow (Fig. 1.3.4).

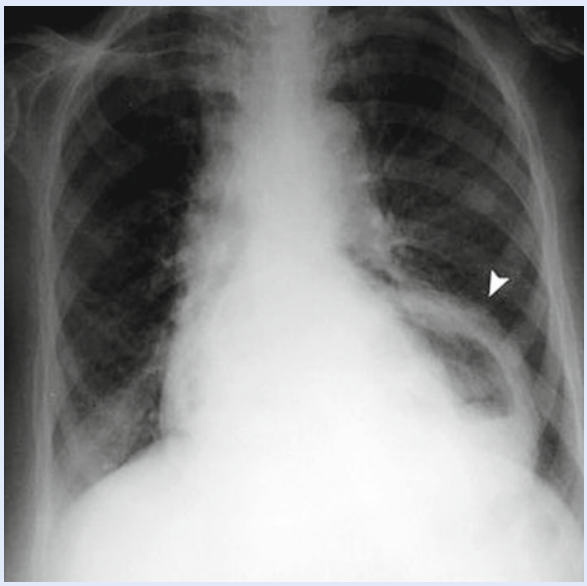

Fig. 1.3.1 Posteroanterior plain chest radiograph shows herniated stomach into the thorax with the gastric bubble observed in the thorax (*arrowhead*)

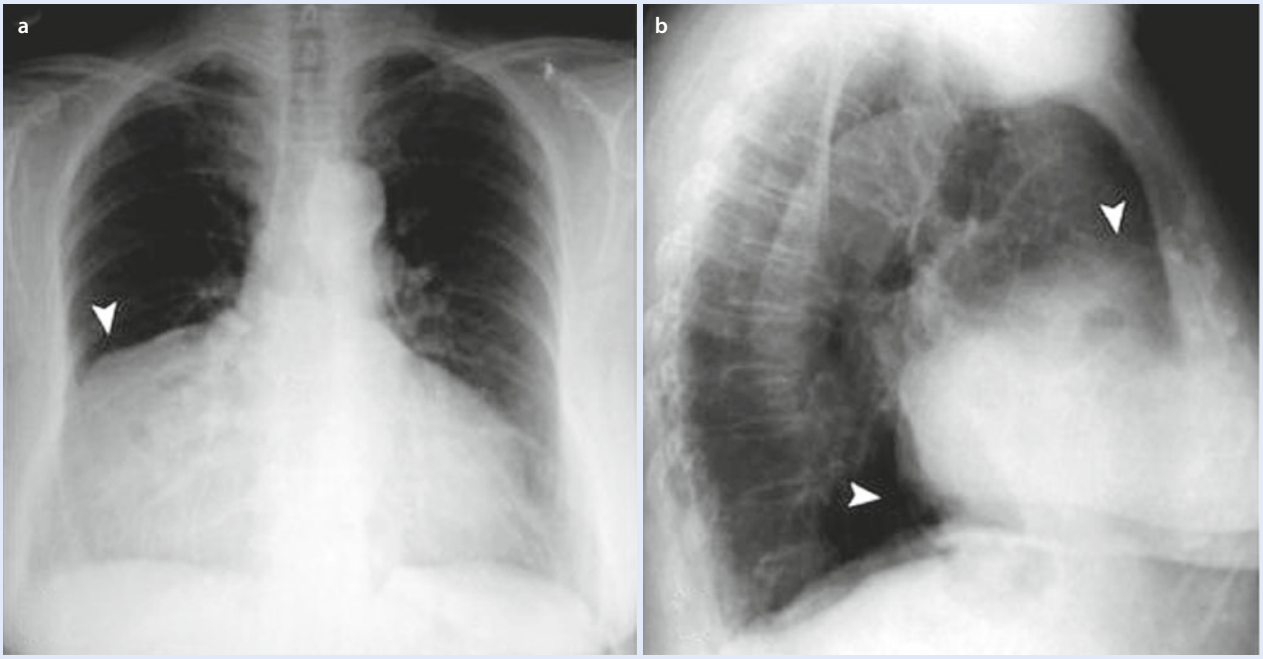

Fig. 1.3.2 Posteroanterior (**a**) and lateral (**b**) plain chest radiographs show right mediastinal mass on (**a**), which is seen located within the anterior/inferior mediastinum on lateral radiographs (*arrows*). The patient is a child, and the mass was omental and bowel herniation due to an anterior congenital diaphragmatic defect (Morgagni hernia)

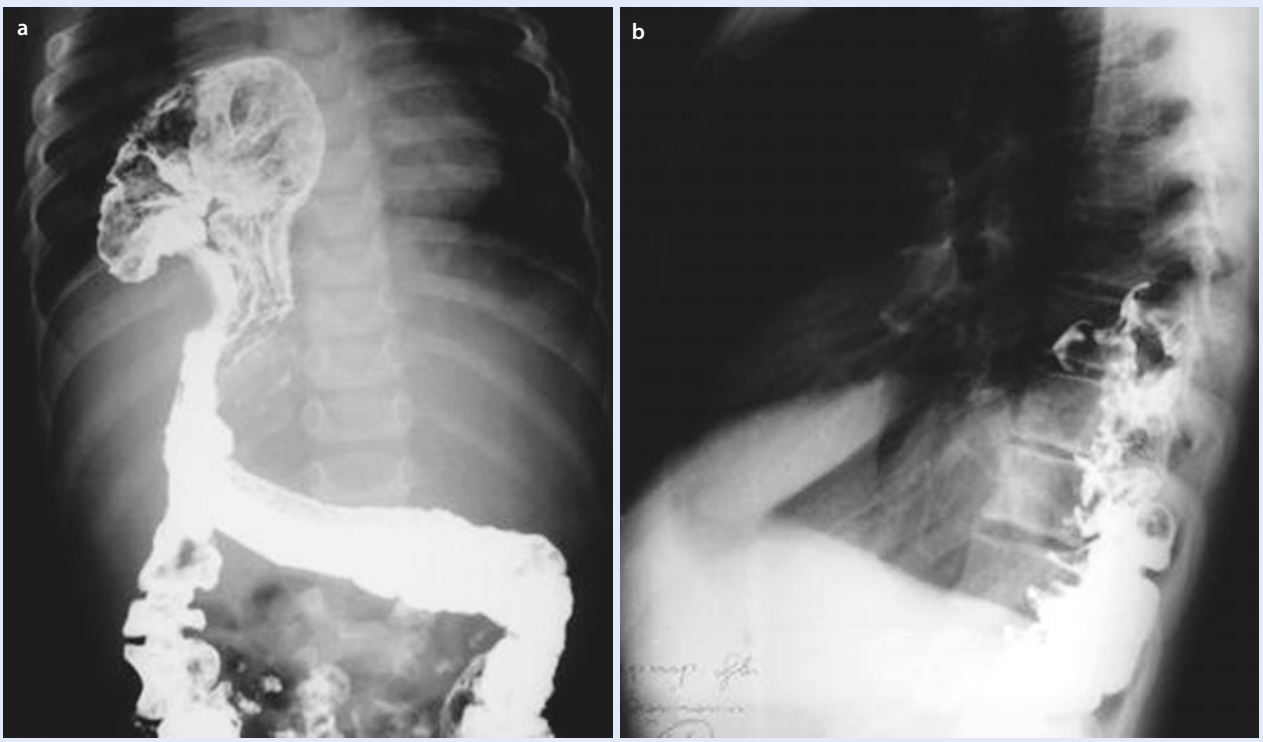

Fig. 1.3.3 Posteroanterior (**a**) and lateral (**b**) barium enema radiographs in a baby with Bochdalek's hernia show herniation of part of the transverse colon through a posterior/inferior diaphragmatic defect (**b**)